

## PAC-1 Activates Procaspase-3 *In Vitro* through Relief of Zinc-Mediated Inhibition

Quinn P. Peterson<sup>1†</sup>, David R. Goode<sup>2†</sup>, Diana C. West<sup>2</sup>,  
Kara N. Ramsey<sup>1</sup>, Joy J. Y. Lee<sup>1</sup> and Paul J. Hergenrother<sup>1,2\*</sup>

<sup>1</sup>Department of Biochemistry,  
Roger Adams Laboratory,  
University of Illinois, Urbana,  
IL 61801

<sup>2</sup>Department of Chemistry,  
Roger Adams Laboratory,  
University of Illinois, Urbana,  
IL 61801

Received 21 November 2008;  
received in revised form  
20 February 2009;  
accepted 3 March 2009  
Available online  
10 March 2009

The direct induction of apoptosis has emerged as a powerful anticancer strategy, and small molecules that either inhibit or activate certain proteins in the apoptotic pathway have great potential as novel chemotherapeutic agents. Central to apoptosis is the activation of the zymogen procaspase-3 to caspase-3. Caspase-3 is the key “executioner” caspase, catalyzing the hydrolysis of a multitude of protein substrates within the cell. Interestingly, procaspase-3 levels are often elevated in cancer cells, suggesting a compound that directly stimulates the activation of procaspase-3 to caspase-3 could selectively induce apoptosis in cancer cells. We recently reported the discovery of a compound, PAC-1, which enhances procaspase-3 activity *in vitro* and induces apoptotic death in cancer cells in culture and in mouse xenograft models. Described herein is the mechanism by which PAC-1 activates procaspase-3 *in vitro*. We show that zinc inhibits the enzymatic activity of procaspase-3 and that PAC-1 strongly activates procaspase-3 in buffers that contain zinc. PAC-1 and zinc form a tight complex with one another, with a dissociation constant of approximately 42 nM. The combined data indicate that PAC-1 activates procaspase-3 *in vitro* by sequestering inhibitory zinc ions, thus allowing procaspase-3 to autoactivate itself to caspase-3. The small-molecule-mediated activation of procaspases has great therapeutic potential and thus this discovery of the *in vitro* mechanism of action of PAC-1 is critical to the development and optimization of other procaspase-activating compounds.

© 2009 Elsevier Ltd. All rights reserved.

Edited by F. Schmid

Keywords: procaspase-3; PAC-1; apoptosis; cancer; zinc

### Introduction

Although general antiproliferative agents that induce death in all rapidly dividing cell types remain the backbone of many chemotherapeutic regimens, recent advances have suggested that “personalized” anticancer strategies hold considerable promise. In personalized medicine, a detailed understanding of the molecular aberrations in the cell is utilized to select a drug with an appropriate mechanism of

action. The potential for such strategies has been powerfully demonstrated for cancers that have translocations, mutations, or aberrant expression levels of key proteins.<sup>1</sup>

One of the hallmarks of cancer is its resistance to apoptosis,<sup>2</sup> a programmed form of cell death important in both the development and maintenance of higher organisms. This resistance enables cancerous cells to survive and divide even in the presence of endogenous proapoptotic stimuli. Morphologically, apoptosis is characterized by cell shrinkage and membrane blebbing, which facilitate the engulfment and recycling of cellular components without provoking the inflammatory response.<sup>3</sup> In human cells, apoptosis occurs through a cascade of events involving two main pathways: the intrinsic pathway and the extrinsic pathway. Both pathways ultimately converge on the activation of the “executioner” procaspases (primarily procaspase-3, but also procaspase-7 and procaspase-6) to caspases, which are

\*Corresponding author. E-mail address:  
hergenro@uiuc.edu.

† These authors contributed equally to this work.

Abbreviations used: EDTA, ethylenediaminetetraacetic acid; DMSO, dimethyl sulfoxide; EGTA, ethylene glycol bis(β-aminoethyl ether) *N,N'*-tetraacetic acid; FITC, fluorescein isothiocyanate; TPEN, *N,N,N',N'*-tetrakis(2-pyridylmethyl)ethylenediamine.

the cysteine proteases that cleave scores of protein substrates within the cell.<sup>4–6</sup> Cancer cells are known to evade apoptosis through a variety of mechanisms involving mutation or altered expression levels of key proteins in the apoptotic cascade,<sup>7,8</sup> including mutation of p53,<sup>9</sup> elevated expression of the anti-apoptotic proteins in the Bcl-2 family,<sup>10</sup> and inactivation of Apaf-1.<sup>11</sup> The net result of these alterations is a resistance to apoptosis, allowing for unchecked cellular proliferation.

In the hopes of reactivating damaged apoptotic cascades and inducing cell death, several proteins in the apoptotic pathway have been targeted by small molecules.<sup>12–14</sup> Indeed, small molecules that disrupt the p53–MDM-2 interaction,<sup>15,16</sup> bind to Bcl-2,<sup>17</sup> promote apoptosome formation,<sup>18</sup> or inhibit XIAP<sup>19,20</sup> have shown potential in cell culture and/or preclinical models of cancer. We embarked on an

effort to bypass the damaged apoptotic cascade in cancer cells and directly activate procaspase-3 to caspase-3 with a small molecule. A procaspase-3 activator would be predicted to induce cell death, and, due to the elevation of procaspase-3 in certain tumor types,<sup>21–26</sup> a procaspase-3-activating compound could have selectivity for killing cancer cells *versus* normal cells. We recently reported the discovery of a compound (called PAC-1, Fig. 1a) that activates procaspase-3 to caspase-3 *in vitro*, induces death in cancer cell lines and cells from primary tumor sample in cell culture, and retards tumor growth *in vivo*.<sup>27</sup> PAC-1 appears to induce death in cancer cells via the direct activation of procaspase-3, as evidenced by both the order and timing of apoptotic events and the correlation of PAC-1 potency with procaspase-3 levels in cancer cells isolated from primary colon tumors.<sup>27</sup>

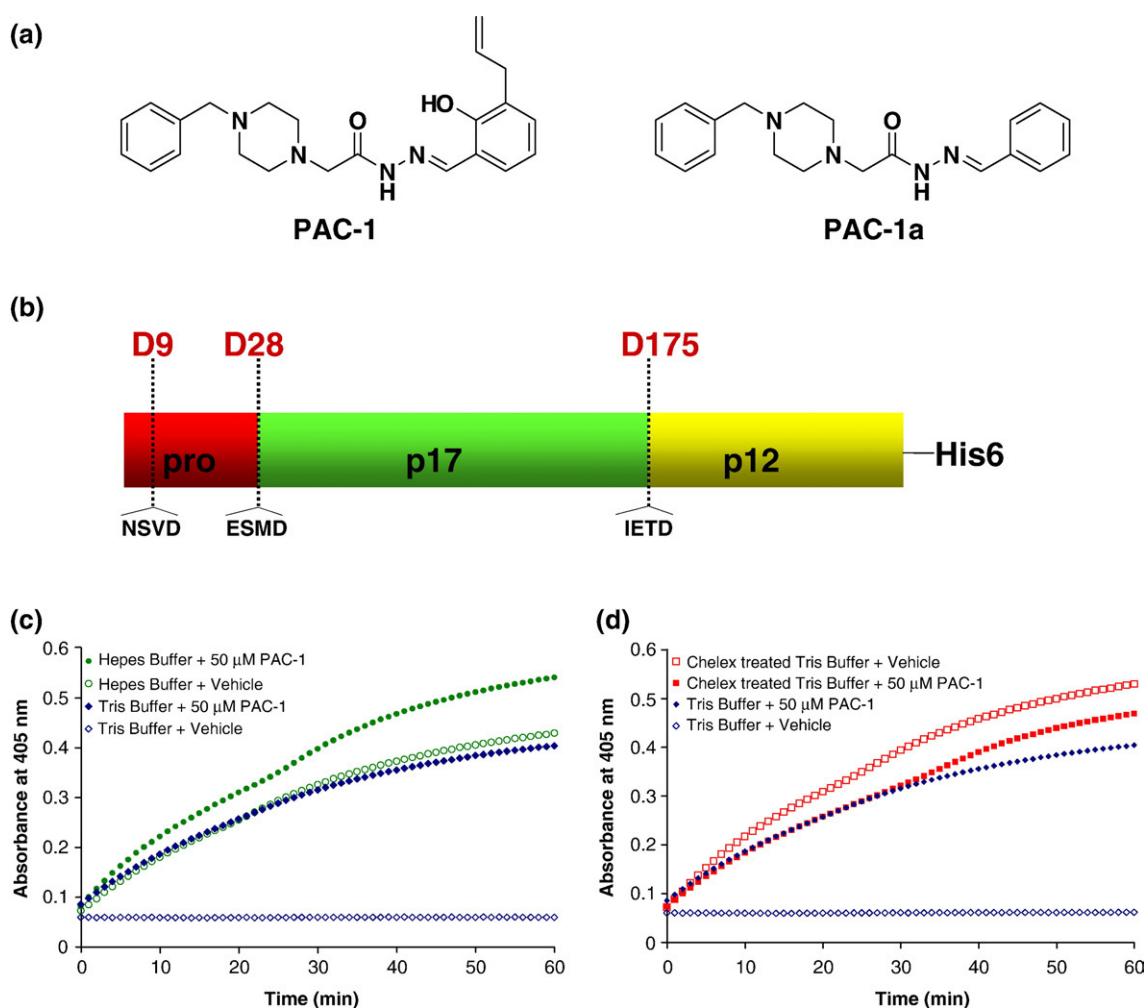


**Fig. 1.** (a) Chemical structures of PAC-1 and PAC-1a. (b) Procaspase-3 can be proteolyzed by caspases or granzymes at D9, D28, or D175. (c) Progress curves reporting on the procaspase-3 processing of the Ac-DEVD-pNA substrate as a function of time. In Tris buffer, procaspase-3 has very little activity on the Ac-DEVD-pNA substrate (open blue diamonds); this activity is dramatically enhanced in the presence of 50  $\mu$ M PAC-1 (closed blue diamonds). The effect of PAC-1 on procaspase-3 activity is much less pronounced in a Hepes buffer (green circles). (d) Progress curves reporting on the procaspase-3 processing of the Ac-DEVD-pNA substrate as a function of time. Treatment of the Tris buffer with a Chelex<sup>®</sup> resin eliminates the activating effect of PAC-1. In a Chelex<sup>®</sup>-treated Tris buffer, the sample containing PAC-1 (closed red squares) has no greater activity over the vehicle-treated controls (open red squares). Shown for comparison is the data for procaspase-3 in Tris buffer that has not been Chelex<sup>®</sup> treated (blue diamonds), the same data as in (c).

This preliminary study indicates that procaspase-3 activation, as well as proenzyme activation in general, could be an important anticancer strategy. However, the precise mechanism by which PAC-1 activates procaspase-3 is unknown. The further development of compounds that induce procaspase activation will be greatly aided by a detailed mechanistic understanding of the PAC-1-induced activation of procaspase-3, and the utility of PAC-1 as a probe in apoptotic research will be significantly enhanced by such information. Described herein are experiments demonstrating that PAC-1 activates procaspase-3 *in vitro* via sequestration of inhibitory zinc ions. Evidence is also presented suggesting that zinc binding is critical to the ability of PAC-1 to induce death in cancer cells in culture. These experiments represent the first detailed look at the *in vitro* mechanism of the PAC-1-mediated activation of procaspase-3 and have implications for both the discovery of other compounds that activate procaspases and for the role of zinc in regulating latent cellular procaspase activity.

## Results

To evaluate the effect of PAC-1 on procaspase-3 *in vitro*, two distinct biochemical assays were utilized. First, caspase-3 enzymatic activity was monitored at 405 nm through the cleavage of the peptidic Ac-DEVD-pNA substrate. Second, the maturation of the procaspase-3 zymogen was tracked by SDS-PAGE. This second method provides a biochemical readout orthogonal to the activity assay and allows direct visualization of procaspase-3 maturation.

Full-length procaspase-3 is composed of an ~4-kDa (28 amino acids) prodomain, a 17-kDa large subunit, and a 12-kDa small subunit (Fig. 1b). While caspase-8 and caspase-9 activate procaspase-3 *in vivo* by proteolysis between the p17 and p12 fragments (at D175), there are two additional sites where procaspase-3 is proteolyzed by caspase/granzyme-related enzymes: between the prodomain and p17 domains (at D28) and inside the prodomain (at D9) (see Fig. 1b).<sup>28,29</sup> *In vitro*, it is known that caspase-3 will cleave procaspase-3 at D9, D28, and D175.<sup>30,31</sup> Interestingly, the procaspase-3 zymogen is itself also catalytically active.<sup>21,30</sup> *In vitro* procaspase-3 will cleave itself to the active caspase-3,<sup>21</sup> and procaspase-3 (either wild-type or the caspase-resistant D9A/D28A/D175A triple mutant) will also process synthetic chromogenic/fluorogenic peptidic caspase-3 substrates.<sup>30</sup> As inferred by studies on the triple mutant, the  $k_{\text{cat}}/K_M$  of procaspase-3 is approximately 200-fold lower than that of caspase-3 on peptidic substrates, with the major effect being a reduction in  $k_{\text{cat}}$ .<sup>30</sup> Thus, *in vitro* procaspase-3 is both an enzyme and a substrate; the cellular relevance of the procaspase-3 enzymatic activity is unknown.

### Buffer dependence of PAC-1-mediated activation of procaspase-3

A starting point for our mechanistic studies was the observation that the *in vitro* activation of

procaspase-3 by PAC-1 varied considerably depending on the buffer composition. Caspases are typically assessed in complex buffers containing multiple components, including ethylenediaminetetraacetic acid (EDTA) and DTT. In such buffers the *in vitro* activating effect of PAC-1 on procaspase-3 is low on an absolute scale, three- to fourfold over background procaspase-3 levels.<sup>27</sup> However, when procaspase-3 activation is assessed in simplified buffers [50 mM Tris, 300 mM NaCl (pH 7.2)] large activation of procaspase-3 by PAC-1 is observed, as demonstrated by the enzyme's ability to cleave the Ac-DEVD-pNA substrate. The progress curves for these experiments are displayed in Fig. 1c; in the Tris-NaCl buffer, procaspase-3 has very little activity, and the activity is greatly enhanced by the addition of PAC-1. Considerably less PAC-1-mediated activation is observed in a Hepes buffer, mostly because procaspase-3 is already quite active in this buffer (Fig. 1c). PAC-1a (Fig. 1a) is a derivative of PAC-1 that had been shown to have no effect on procaspase-3 activation *in vitro* and no death-inducing effect on cultured cancer cells.<sup>27</sup> In accord with this previous finding, PAC-1a had no activating effect in any of the buffer conditions in Fig. 1c (see Supporting Information). It had been shown that caspase-3 and certain other caspases are inhibited by the divalent metal ion zinc.<sup>32–36</sup> Given the known ability of *o*-hydroxy *N*-acyl hydrazones (such as contained within PAC-1) to chelate metals,<sup>37</sup> we began to suspect that an interaction of PAC-1 with a divalent metal in the assay buffer could be part of its mechanism of action. We thus set out to test the hypothesis that PAC-1 activates procaspase-3 via sequestration of inhibitory metals.

### Metal removal abolishes the activating effect of PAC-1

Aqueous buffers can be treated with commercial resins that will bind to and remove divalent metal ions. One such resin is Chelex<sup>®</sup>, polystyrene beads that display imidoacetate functional groups. Chelex<sup>®</sup> will bind tightly to divalent transition metals and poorly to smaller cations; treatment of a buffer at 5 g Chelex<sup>®</sup> per 100 mL for 1 h quantitatively removes transition metals. The ability of PAC-1 to activate procaspase-3 was thus assessed before and after treatment of the Tris-NaCl buffer with the Chelex<sup>®</sup> resin. As shown by the progress curves in Fig. 1d, in the Chelex<sup>®</sup>-treated buffer, procaspase-3 has considerable activity, and the addition of PAC-1 has no activating effect and is in fact slightly inhibitory. PAC-1a also had no activating effect in any of the buffer conditions in Fig. 1d (see Supporting Information).

### Caspase-3 and procaspase-3 are inhibited by divalent metals

To further probe the metal dependence of PAC-1 activity, we examined the effect of various metal ions on caspase-3 activity. As shown by the graph in

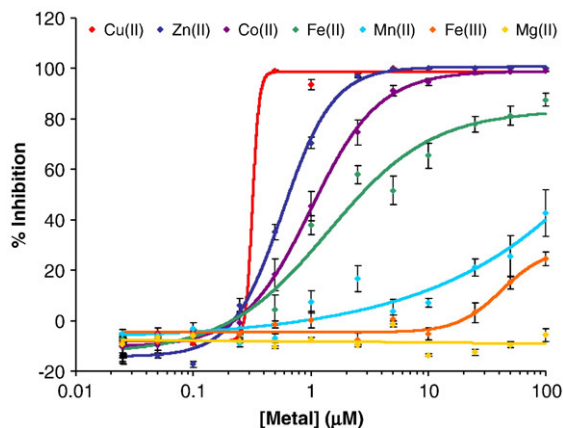


**Fig. 2.** The effect of various metal ions on the catalytic activity of caspase-3.  $\text{CuSO}_4$ ,  $\text{ZnSO}_4$ ,  $\text{CoCl}_2$ ,  $\text{FeCl}_2$ ,  $\text{MnCl}_2$ ,  $\text{FeCl}_3$ , and  $\text{MgCl}_2$  were added to caspase-3 (500 nM) over the given concentration range. The activity of caspase-3 was then assessed by monitoring the cleavage of the Ac-DEVD-pNA substrate. Error bars represent standard error.

**Fig. 2.**  $\text{Zn}^{2+}$  and  $\text{Co}^{2+}$  are both potent inhibitors of caspase-3 activity. Substoichiometric levels of  $\text{Cu}^{2+}$  appear to inhibit caspase-3, perhaps not surprising given the known redox chemistry of this metal and the importance of the active-site sulfhydryl in caspase-3. Other metal ions (manganese, iron, and magnesium) had a lesser effect on caspase-3 inhibition. The data for caspase-3 and  $\text{Zn}^{2+}$  are consistent with data in the literature,<sup>32,33</sup> while, to our knowledge, the effect of other metal ions on caspase-3 activity has not been previously reported. Thus, the variable activity of PAC-1 in different buffers (Fig. 1c and d) can be explained by the presence of metal ions in those buffers. For example, our inductively coupled plasma mass spectrometry analysis of the Trizma base (minimum 99% titration purity, from Sigma, analyzed as a solid) showed that a 50 mM Tris buffer made from this solid contains 100 nM zinc, 0.3 nM copper, 780 nM iron, and 250 nM cobalt.

Although 90% of cellular zinc is believed to be sequestered in tightly bound complexes within proteins (metalloenzymes, zinc fingers, etc.), it is believed that approximately 10% of zinc exists in labile, loosely bound pools.<sup>38</sup> Given that zinc appears to be the most physiologically relevant metal of those inhibitors identified in Fig. 2, we choose to focus on zinc. The effect of a range of concentrations of zinc on caspase-3 and procaspase-3 enzymatic activity was examined. All buffers were first treated with Chelex<sup>®</sup> resin to remove any trace metal contaminants. As procaspase-3 will slowly autoproteolyze itself to active caspase-3, we also created the triple mutant of procaspase-3 in which all three caspase cleavage sites have been removed (D9A/D28A/D175A). Consistent with data in the literature,<sup>30</sup> this procaspase-3 triple mutant is proteolytically stable and has activity ~200-fold less than that of caspase-3 (data not shown). Enzyme assays in the presence of zinc indicate that this metal

powerfully inhibits caspase-3 (Fig. 3a), procaspase-3 (Fig. 3b), and the procaspase-3(D9A/D28A/D175A) mutant (Fig. 3c). Because procaspase-3 is considerably less active than caspase-3, a higher concentration of the procaspase-3(D9A/D28A/D175A) mutant was used in these experiments. To the best of our knowledge, this is the first demonstration that zinc inhibits procaspase-3 activity *in vitro*.

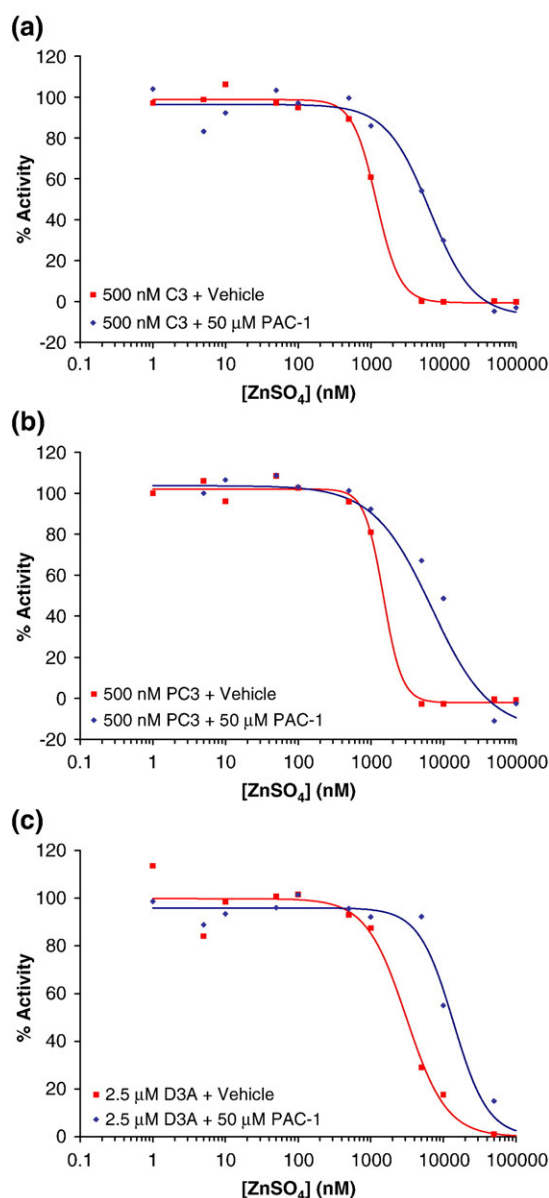


**Fig. 3.** (a) As assessed by the cleavage of the Ac-DEVD-pNA substrate, the ability of zinc to inhibit caspase-3 (C3, 500 nM) activity *in vitro* is reduced in the presence of PAC-1 (50  $\mu\text{M}$ ). (b) As assessed by the cleavage of the Ac-DEVD-pNA substrate, the ability of zinc to inhibit procaspase-3 (PC3, 500 nM) activity *in vitro* is reduced in the presence of PAC-1 (50  $\mu\text{M}$ ). (c) As assessed by the cleavage of the Ac-DEVD-pNA substrate, the ability of zinc to inhibit the procaspase-3(D9A/D28A/D175A) mutant (D3A, 2.5  $\mu\text{M}$ ) activity *in vitro* is reduced in the presence of PAC-1 (50  $\mu\text{M}$ ). Data shown are representative of three trials.

### PAC-1 addition reactivates zinc-inhibited caspase-3 and procaspase-3

Experiments were also conducted to assess the ability of PAC-1 to relieve the zinc-mediated inhibition of caspase-3 and procaspase-3 activity. A concentration of 50  $\mu\text{M}$  PAC-1 was used for these experiments. The results from these experiments are displayed in Fig. 3a, b, and c for caspase-3, procaspase-3, and the procaspase-3(D9A/D28A/D175A) mutant, respectively. PAC-1 relieves the zinc-mediated inhibition of caspase-3, procaspase-3, and the procaspase-3(D9A/D28A/D175A) mutant, as indicated by the shift in the  $\text{ZnSO}_4$  inhibition curves in the presence of PAC-1 (Fig. 3a–c).

### PAC-1 activates procaspase-3 and caspase-3 in a dose-dependent manner

Next, the ability of PAC-1 to activate procaspase-3 and caspase-3 in a dose-dependent manner was assessed in the presence and absence of zinc. For these experiments, concentrations of PAC-1 from 0.025 to 100  $\mu\text{M}$  were evaluated, and all buffers were treated with Chelex<sup>®</sup> resin prior to addition of PAC-1 or zinc. The results of these experiments are displayed in Fig. 4a–c, for caspase-3, procaspase-3, and the procaspase-3(D9A/D28A/D175A) mutant, respectively. As expected, in the presence of zinc and very low concentrations of PAC-1, the procaspase-3/caspase-3 enzymes are powerfully inhibited. However, as PAC-1 concentration is increased, the activity of the enzymes in the buffer containing zinc is increased to 40–60% of the maximal rate (i.e., the rate of the enzyme in the absence of zinc). Interestingly, very high concentrations of PAC-1 actually inhibit the enzymes. Experiments analogous to those presented in Fig. 4a–c show that PAC-1a had no activating effect on caspase-3, procaspase-3, and the procaspase-3(D9A/D28A/D175A) triple mutant (see [Supporting Information](#)).

### PAC-1 activates caspase-3 to cleave procaspase-3

As mentioned, caspase-3 will cleave procaspase-3 *in vitro*, a process that is easily observed by SDS-PAGE.<sup>30,31</sup> In addition, the automaturation of procaspase-3 has also been observed *in vitro* by SDS-PAGE.<sup>21</sup> Based on our above results in the activity assay, we predicted that zinc would inhibit the procaspase-3 cleavage by caspase-3, and the procaspase-3 automaturation, and that this inhibition would be relieved by PAC-1. A potential complication in the analysis is that wild-type procaspase-3 is both the substrate and the enzyme in these automaturation experiments. In order to separate these two roles, the procaspase-3(D9A/D28A/D175A) triple mutant was utilized as the version that functions solely as the enzyme (i.e., it cannot be cleaved by caspases), and procaspase-3(C163A) was utilized as the version that functions solely

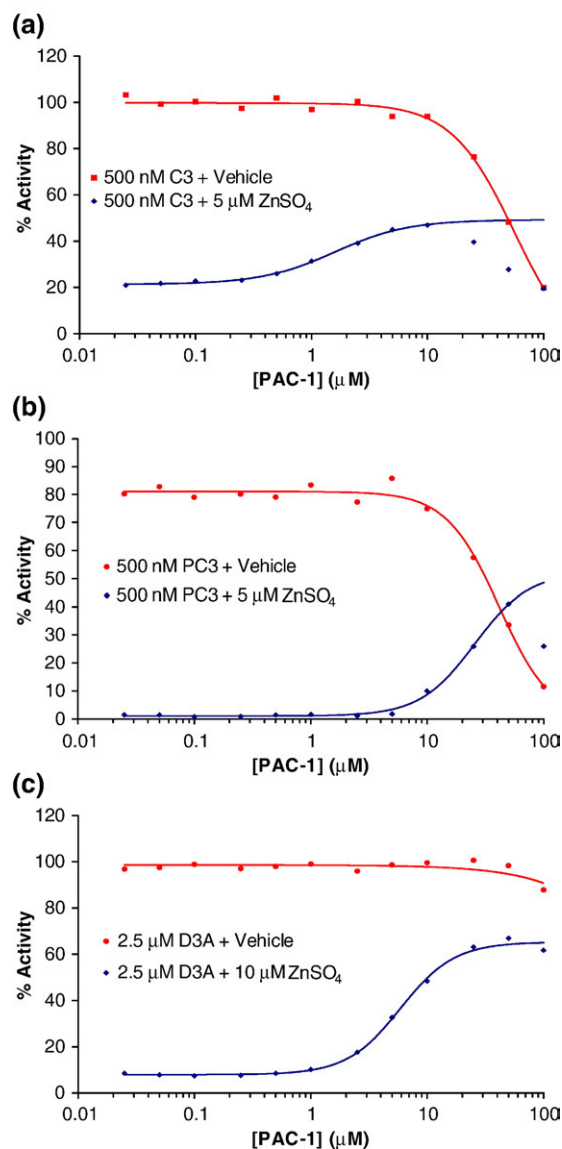


**Fig. 4.** (a) PAC-1 enhances caspase-3 (C3) activity when assayed in a buffer containing 5  $\mu\text{M}$   $\text{ZnSO}_4$ . (b) PAC-1 enhances procaspase-3 (PC3) activity when assayed in a buffer containing 5  $\mu\text{M}$   $\text{ZnSO}_4$ . (c) PAC-1 enhances the procaspase-3(D9A/D28A/D175A) (D3A) mutant activity when assayed in a buffer containing 5  $\mu\text{M}$   $\text{ZnSO}_4$ . As shown in (a), (b), and (c), PAC-1 actually inhibits these three enzymes at high compound concentrations. Data shown are representative of three trials.

as the substrate. The mutation of the active-site cysteine 163 of caspase-3/procaspase-3 abolishes catalytic activity;<sup>39–42</sup> thus, this protein can still be cleaved by caspases, but itself has no enzymatic activity.

To assess the effect of zinc and PAC-1 on the ability of caspase-3 to cleave procaspase-3, procaspase-3(C163A) was incubated with caspase-3 for defined periods of time. As shown in Fig. 5a, in the absence of zinc caspase-3 will process procaspase-3 (C163A) in this *in vitro* experiment, consistent with the data in the literature.<sup>30,31</sup> As shown in Fig. 5b,

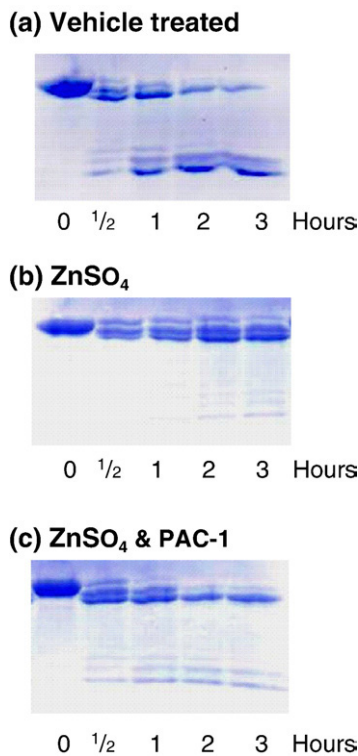


**Fig. 5.** Zinc inhibits the ability of caspase-3 to cleave procaspase-3, an effect that is relieved by addition of PAC-1. (a) Procaspase-3 (C163A) (50  $\mu$ M) was incubated with caspase-3 (10  $\mu$ M). (b) Procaspase-3 (C163A) (50  $\mu$ M) was incubated with caspase-3 (10  $\mu$ M) and ZnSO<sub>4</sub> (50  $\mu$ M). (c) Procaspase-3 (C163A) (50  $\mu$ M) was incubated with caspase-3 (10  $\mu$ M), ZnSO<sub>4</sub> (50  $\mu$ M), and 50  $\mu$ M PAC-1 (50  $\mu$ M). Samples were analyzed by SDS-PAGE and Coomassie staining.

this processing is greatly inhibited by the addition of zinc. Finally, as shown in Fig. 5c, addition of PAC-1 restores the ability of caspase-3 to cleave procaspase-3 (C163A). This is shown both by the appearance of the p12 and p17 active fragments and by the processing of procaspase-3 (C163A) to successively shorter forms. During *in vitro* activation of procas-

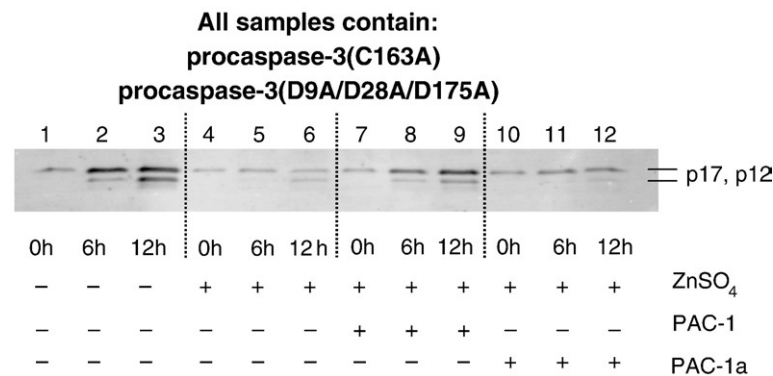


**Fig. 6.** Zinc inhibits the ability of procaspase-3 to cleave another molecule of procaspase-3, an effect that is relieved by addition of PAC-1. Procaspase-3(D9A/D28A/D175A) (10  $\mu$ M) was incubated with procaspase-3 (C163A) (50  $\mu$ M) (lanes 1–3) and 100  $\mu$ M ZnSO<sub>4</sub> (lanes 4–6) or 100  $\mu$ M ZnSO<sub>4</sub> and 50  $\mu$ M PAC-1 (lanes 7–9) for up to 12 h at 37 °C. Samples were analyzed by SDS-PAGE and Western blotting using polyclonal antibody against the p12 and p17 caspase-3 fragments. In the absence of zinc, procaspase-3(D9A/D28A/D175A) processes the procaspase-3 (C163A) substrate within 12 h. In the presence of zinc, this automaturization is inhibited (lanes 4–6), an effect that is relieved by the addition of PAC-1 (lanes 7–9), but not PAC-1a (lanes 10–12).

pase-3 by caspase-3, it is known that the cleavage is such that bands are observed corresponding to the full-length procaspase-3 (~34 kDa), the  $\Delta$ 1–9 procaspase-3 (~32 kDa), and the  $\Delta$ 1–28 procaspase-3 (~30 kDa), in addition to the active caspase-3 fragments;<sup>30,31</sup> this can be observed in the gels in Fig. 5.

**PAC-1 induces procaspase-3 automaturization**

To investigate the effect of zinc and PAC-1 on the ability of procaspase-3 to autoactivate itself to caspase-3, an experiment was devised whereby procaspase-3(C163A) was used as the protein substrate and procaspase-3(D9A/D28A/D175A) was used as the enzyme. In the event, procaspase-3 (C163A) (50  $\mu$ M) was incubated with procaspase-3 (D9A/D28A/D175A) (10  $\mu$ M) in the presence or absence of zinc and PAC-1, for 0, 6, and 12 h. The lowered catalytic activity of procaspase-3 produces only low levels of product in these experiments; thus, detection was performed by Western blotting. When procaspase-3(C163A) is incubated with procaspase-3 (D9A/D28A/D175A), caspase-3 p17 and p12 fragments are observed within 12 h (Fig. 6, lanes 1–3). Running this same experiment in the presence of zinc significantly inhibits zymogen processing (Fig. 6, lanes 4–6). However, upon addition of PAC-1, an increase in the levels of the processed fragments is once again observed (Fig. 6, lanes 7–9); PAC-1a has no such effect (Fig. 6, lanes 10–12). This experiment demonstrates that PAC-1 enhances the activity of the procaspase-3 zymogen, allowing it to cleave another molecule of procaspase-3. In the cell, of course, active caspase-3 would be generated through this process, and PAC-1 could then also enhance the activity of caspase-3 as part of a feed-forward cycle.

**PAC-1 addition reactivates zinc-inhibited caspase-7 and procaspase-7**

Caspase-7 is another major cellular executioner caspase and it shares a high degree of structural homology with caspase-3.<sup>43,44</sup> Similar to procaspase-3, the procaspase-7 zymogen is expressed with a short prodomain (23 amino acids) followed by large

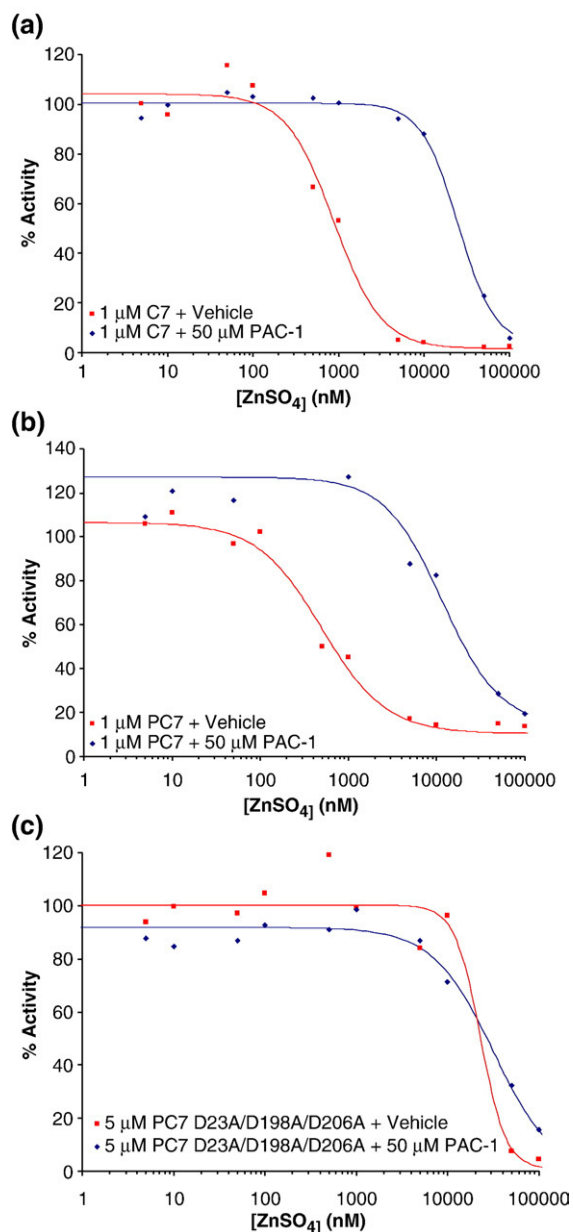


**Fig. 7.** (a) As assessed by the cleavage of the Ac-DEVD-pNA substrate, the ability of zinc to inhibit caspase-7 (C7, 1  $\mu$ M) activity *in vitro* is reduced in the presence of PAC-1 (50  $\mu$ M). (b) As assessed by the cleavage of the Ac-DEVD-pNA substrate, the ability of zinc to inhibit procaspase-7 (PC7, 1  $\mu$ M) activity *in vitro* is reduced in the presence of PAC-1 (50  $\mu$ M). (c) As assessed by the cleavage of the Ac-DEVD-pNA substrate, the ability of zinc to inhibit the procaspase-7(D23A/D198A/D206A) mutant (5  $\mu$ M) activity *in vitro* is reduced in the presence of PAC-1 (50  $\mu$ M). Data shown are representative of at least three trials.

and small subunits.<sup>45</sup> Similar to procaspase-3, procaspase-7 is activated by upstream initiator caspases,<sup>46,47</sup> and caspase-7 is inhibited by zinc.<sup>33</sup> Experiments were thus conducted to assess the ability of PAC-1 to relieve the zinc-mediated inhibition of caspase-7 and procaspase-7 activity. A concentration of 50  $\mu$ M PAC-1 was used for these

experiments. The results from these experiments are displayed in Fig. 7a, b, and c for caspase-7, procaspase-7, and the procaspase-7(D23A/D198A/D206A) mutant, respectively. The triple mutant of procaspase-7 was created to render this zymogen resistant to caspase-mediated proteolysis; this mutant protein has the aspartic acids of two canonical caspase cleavage sites altered (D23 and D198), in addition to a third site (D206) that is known to be a substrate for further processing.<sup>44,48,49</sup> Analysis of this triple mutant by SDS-PAGE shows it to be fully

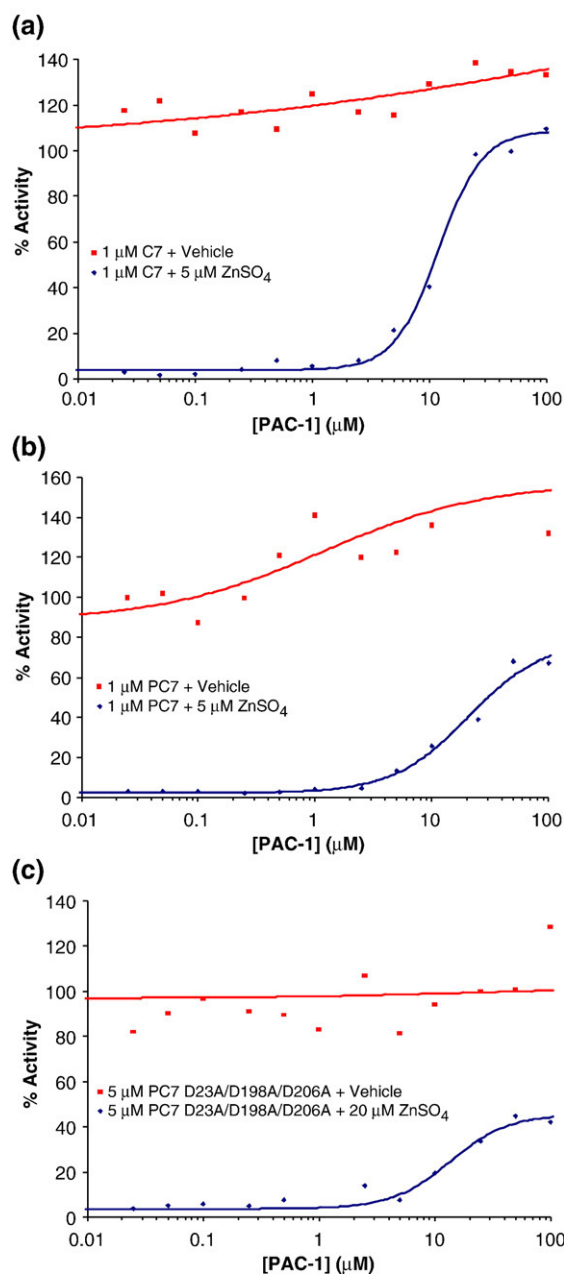


**Fig. 8.** (a) PAC-1 enhances caspase-7 (C7) activity when assayed in a buffer containing 5  $\mu$ M  $ZnSO_4$ . (b) PAC-1 enhances procaspase-7 (PC7) activity when assayed in a buffer containing 5  $\mu$ M  $ZnSO_4$ . (c) PAC-1 enhances the procaspase-7(D23A/D198A/D206A) mutant activity when assayed in a buffer containing 20  $\mu$ M  $ZnSO_4$ . Data shown are representative of at least three trials.

stable over the course of 8 h. This procaspase-7 (D23A/D198A/D206A) mutant is thus analogous to the procaspase-3(D9A/D28A/D175A) triple mutant and provides a version of procaspase-7 that is stable during the time course of the biochemical experiments described herein. PAC-1 relieves the zinc-mediated inhibition of caspase-7, procaspase-7, and the procaspase-7(D23A/D198A/D206A) mutant, as indicated by the shift in the  $\text{ZnSO}_4$  inhibition curves in the presence of PAC-1 (Fig. 7a–c). To the best of our knowledge, this is the first demonstration that zinc inhibits procaspase-7 activity *in vitro*.

### PAC-1 activates procaspase-7 and caspase-7 in a dose-dependent manner

In analogy to our experiments with procaspase-3/caspase-3 (Fig. 4), the ability of PAC-1 to activate procaspase-7 and caspase-7 in a dose-dependent manner was assessed in the presence and absence of zinc. For these experiments, concentrations of PAC-1 from 0.025 to 100  $\mu\text{M}$  were evaluated, and all buffers were treated with Chelex<sup>®</sup> resin prior to addition of PAC-1 or zinc. The results of these experiments are displayed in Fig. 8a–c, for caspase-7, procaspase-7, and the procaspase-7(D23A/D198A/D206A) mutant, respectively. As expected, in the presence of zinc and very low concentrations of PAC-1, the procaspase-7 and caspase-7 enzymes are powerfully inhibited. However, as PAC-1 concentration is increased, the activity of the enzymes in the buffer containing zinc is increased to 40–100% of the maximal rate (i.e., the rate of the enzyme in the absence of zinc). Interestingly, in contrast to the data with procaspase-3/caspase-3, very high concentrations of PAC-1 do not inhibit the procaspase-7/caspase-7 enzymes.

### PAC-1 binds tightly to $\text{Zn}^{2+}$

Although compounds containing the *o*-hydroxy *N*-acyl hydrozone motif have been shown to bind to metals,<sup>50</sup> some of these compounds do not bind  $\text{Zn}^{2+}$  tightly and instead have  $K_d$  values in the micromolar range.<sup>51</sup> We thus set out to determine the affinity of PAC-1 for zinc. As shown in Fig. 9a, titration of PAC-1 with increasing amounts of  $\text{ZnSO}_4$  results in a change in the UV–visible spectrum of this compound. This shift in molar absorptivity upon  $\text{Zn}^{2+}$  binding provides a convenient method to determine both the stoichiometry of PAC-1– $\text{Zn}^{2+}$  binding and the dissociation constant of this interaction.

A modified version of the method of continuous variations was used for this determination.<sup>52</sup> The absorbance at 410 nm was acquired for various mole fractions of  $\text{ZnSO}_4$  and PAC-1 with a total concentration of 50  $\mu\text{M}$ . These values were then normalized *versus* the maximal absorbance possible at the stoichiometric point (i.e., when all of the  $\text{Zn}^{2+}$  is bound by excess PAC-1), which was set as 1. Application of the continuous variations method revealed that PAC-1 binds  $\text{Zn}^{2+}$  in a 1:1 stochio-

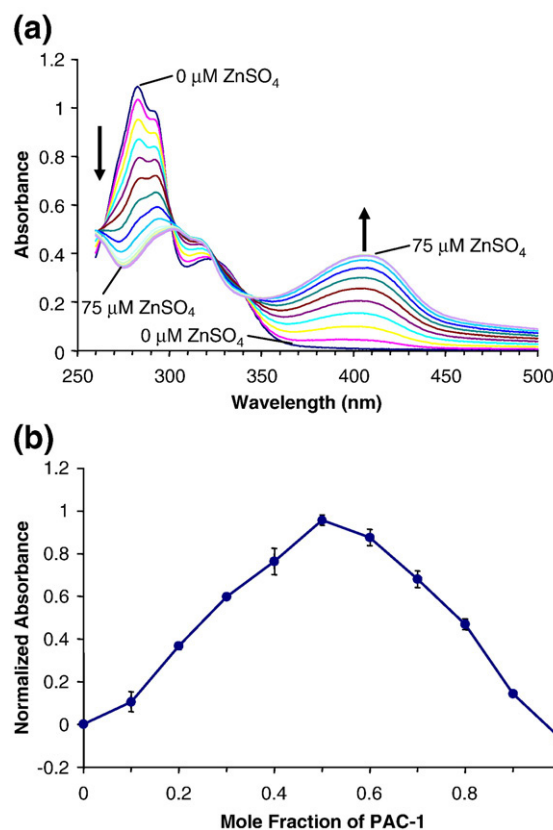


**Fig. 9.** (a) Titration of  $\text{ZnSO}_4$  into a solution of PAC-1 (50  $\mu\text{M}$  in 50 mM HEPES, 100 mM  $\text{KNO}_3$ , pH 7.2 buffer) causes a change in the UV–visible spectra of PAC-1. Shown are  $\text{ZnSO}_4$  concentrations of 0 to 75  $\mu\text{M}$  in 5  $\mu\text{M}$  increments. (b) Analysis of the PAC-1– $\text{Zn}^{2+}$  binding interaction and stoichiometry by the continuous variations method. Based on the location of the peak value, the stoichiometry was determined to be 1:1, and the  $K_d$  was determined to be 42 nM. Error bars represent standard deviation from the mean.

metry, as evidenced by the peak at 0.5 mol fraction in the graph in Fig. 9b. Also apparent from Fig. 9b is the very strong nature of this small molecule–metal interaction. At the 1:1 stoichiometry, PAC-1 has almost entirely shifted its absorption to the zinc-bound state (96% of PAC-1 is  $\text{Zn}^{2+}$  bound at a 1:1 ratio of PAC-1– $\text{Zn}^{2+}$ ). Using this 96% value and the equation  $\log K_a = 0.3010 - \log M + \log y_{\text{max}} - 2 \log (1 - y_{\text{max}})$ , we obtain a  $K_d = 42$  nM for the PAC-1– $\text{Zn}^{2+}$  interaction. While the  $K_d$  for the PAC-1– $\text{Zn}^{2+}$  interaction is 42 nM, as shown in Fig. 9a, an absorbance change is still observed with micromolar concentrations of zinc. This is due to the high concentration of total ligand (50  $\mu\text{M}$ ) in this experiment relative to the  $K_d$ . Based on the concentrations of zinc and PAC-1 utilized in this experiment, the Adair equation<sup>53</sup> predicts a half-maximal population average site occupancy for the PAC-1– $\text{Zn}^{2+}$  complex at  $\sim 30$   $\mu\text{M}$  zinc, consistent with the data obtained (Fig. 9a). Titration of  $\text{ZnSO}_4$  into PAC-1a gave no spectral change as monitored by UV–vis spectroscopy, consistent with the notion

that PAC-1a does not bind  $Zn^{2+}$  (see [Supporting Information](#)).

To confirm this result, a second method was used to determine the PAC-1– $Zn^{2+}$  dissociation constant. In this experiment, a preformed complex of PAC-1 and  $Zn^{2+}$  was titrated with EGTA [ethylene glycol bis( $\beta$ -aminoethyl ether)  $N,N'$ -tetraacetic acid, a metal binder with a known affinity for  $Zn^{2+}$ ], and the absorbance at 410 nm was monitored (see [Supporting Information](#)). Using the literature value for the EGTA– $Zn^{2+}$  association constant,<sup>54</sup> we calculated the PAC-1– $Zn^{2+}$  dissociation constant as 55 nM, in general agreement with  $K_d$  of 42 nM calculated through the method of continuous variations.

### Induction of apoptotic cell death by PAC-1 is inhibited by $Zn^{2+}$

Although the goal of this study was to determine the mechanism by which PAC-1 activates procaspase-3 *in vitro*, we have also conducted preliminary experiments investigating the relevance of this mechanism to the death-inducing effect of PAC-1 in cell culture. Thus, the effect of exogenous zinc on the ability of PAC-1 to induce apoptotic death in cancer cells in culture was assessed. For this experiment, U-937 cells (human lymphoma cell line) were incubated with vehicle,  $ZnSO_4$  (100  $\mu$ M), etoposide (10  $\mu$ M), etoposide plus  $ZnSO_4$ , PAC-1 (50  $\mu$ M), and PAC-1 plus  $ZnSO_4$ ; after 24 h, apoptotic cell death was assessed by fluorescein isothiocyanate (FITC)–Annexin V and propidium iodide staining and flow cytometry. Apoptotic cells are those that stain positive for FITC–Annexin V, but negative for propidium iodide. The results of this experiment are displayed in [Fig. 10](#). Treatment of cells with vehicle or with  $ZnSO_4$  induces little apoptosis, whereas treatment with etoposide induces apoptosis in almost 70% of the cells, a value that is not significantly reduced by the presence of  $ZnSO_4$ . In contrast, the apoptotic death induced by PAC-1 is significantly reduced by the addition of  $ZnSO_4$ . Comparison of the etoposide and PAC-1 data suggests that the  $ZnSO_4$ -mediated inhibition of the PAC-1 cytotoxicity is not merely a consequence of a general antiapoptotic effect of  $ZnSO_4$ .

## Discussion

The data presented in this manuscript demonstrate that PAC-1 activates procaspase-3 *in vitro* through the sequestration of inhibitory metals. While it had been previously shown that modest levels of activation of procaspase-3 (and no activation of caspase-3) by PAC-1 are observed in complex buffer systems,<sup>27</sup> we now show that in buffers consisting simply of Tris and NaCl, powerful PAC-1-mediated activation of procaspase-3 and caspase-3 is observed. Treatment of these buffers with Chelex<sup>®</sup> removes inhibitory divalent metals, allowing the enzymes to be fully active and thus

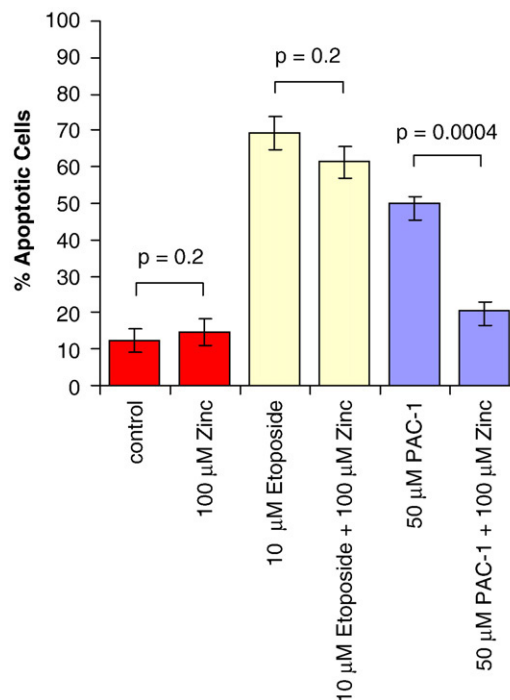


**Fig. 10.** PAC-1 induces apoptosis in U937 cells, an effect that is reduced in the presence of  $ZnSO_4$ . U937 cells were treated with the indicated concentrations of PAC-1 and/or  $ZnSO_4$  for 24 h, at which point cell death was assessed by Annexin V/propidium iodide staining and flow cytometry. As also shown,  $ZnSO_4$  has little effect on the toxicity of etoposide in the same assay. Error bars represent standard error;  $n=3$ .

abolishing the PAC-1-mediated activation. Consistent with this hypothesis is the fact that PAC-1 binds quite tightly to zinc, with a  $K_d=42$  nM. A structurally related compound that does not bind zinc, PAC-1a, does not activate procaspase-3 *in vitro* and does not induce death of cancer cells in culture.

Also reported herein is the first *in vitro* demonstration that the catalytic activity of procaspase-3 is inhibited by zinc. We show that zinc will inhibit the procaspase-3-catalyzed processing of peptidic substrates ([Figs. 3b and 4b](#)) and the autoactivation of procaspase-3, where the enzymatic and the substrate properties of procaspase-3 were bifurcated ([Fig. 6](#)). As wild-type procaspase-3 can be contaminated with active caspase-3, the D9A/D28A/D175A triple mutant of procaspase-3 was created and evaluated; this mutant is known to be fully resistant to caspase cleavage.<sup>30</sup> More importantly, experiments with this triple mutant of procaspase-3 show that zinc is also an inhibitor of this enzyme ([Figs. 3c and 4c](#)), and in the presence of zinc, PAC-1 is able to enhance the activity of this mutant against both peptidic ([Figs. 3c and 4c](#)) and protein ([Fig. 6](#)) substrates. The mechanism of PAC-1-mediated activation of procaspase-3 *in vitro* that thus emerges from this work is shown in [Fig. 11](#): PAC-1 binds to zinc, allowing procaspase-3 to be enzymatically active

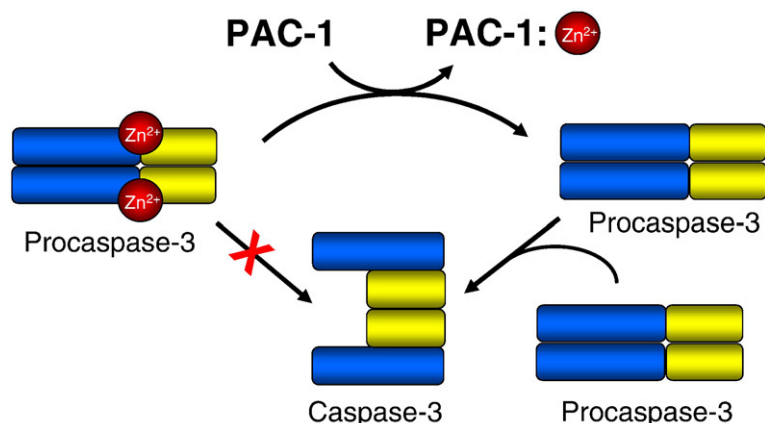


**Fig. 11.** The proposed mechanism for the PAC-1-induced activation of procaspase-3 *in vitro*. Zinc inhibits the catalytic activity of procaspase-3. PAC-1 binds tightly to zinc, and thus relieves the zinc-mediated inhibition of procaspase-3. This zinc sequestration enables procaspase-3 to function as an enzyme and proteolytically cleave another molecule of procaspase-3, converting it to caspase-3.

and to subsequently activate another molecule of procaspase-3 to form caspase-3.

We also present data consistent with the notion that PAC-1 induces death in cultured cancer cells through the activation of procaspase-3 by metal sequestration, as pretreatment of PAC-1 with zinc reduces the ability of PAC-1 to induce apoptotic death in U-937 cells (Fig. 10). It is of course possible that exogenous zinc is simply binding to PAC-1 and preventing it from entering the cell. Minimally, the data in Fig. 10 suggest that PAC-1 is capable of binding zinc in cell culture media. More importantly, this experiment, together with *in vitro* data for PAC-1a, demonstrates a direct correlation between the cytotoxic potential of PAC-1 and its ability to bind zinc. Additionally, zinc has been previously shown to co-localize with procaspase-3 inside cells.<sup>38,55</sup> Based on the zinc–procaspase-3 co-localization data and other data, it has been previously suggested that zinc binds to and inhibits procaspase-3 inside the cell.<sup>38,56</sup> Although more experiments are required to determine the mechanism by which PAC-1 induces death in cancer cells in culture, these data, combined with our *in vitro* data showing PAC-1-mediated activation of procaspase-3 by metal sequestration, lead us to the following hypothesis: PAC-1 enters cells where, with a  $K_d$  of 42 nM, it competes favorably for the labile zinc pool to reduce the levels of zinc available to inhibit procaspase-3, thus resulting in procaspase-3 autoactivation to caspase-3. Once caspase-3 is generated it can activate more procaspase-3, caspase-3 substrates are cleaved, and apoptosis occurs.

Examination of the literature lends ample support to this hypothesis. There are multiple reports that describe the ability of zinc chelators to induce apoptosis.<sup>57</sup> Perhaps the most detailed and convincing studies have been performed with the zinc chelator *N,N,N',N'*-tetrakis(2-pyridylmethyl)ethylenediamine (TPEN). In several different cell lines and systems, TPEN has been found to strongly induce apoptosis.<sup>58–62</sup> Other studies have shown that small changes to the labile zinc content of the cell make cells more susceptible to apoptosis.<sup>63</sup> In light of the *in vitro* data presented herein with PAC-1 and the evidence showing that procaspase-3 is inhibited by

zinc, TPEN may be exerting its proapoptotic effect in a manner similar to that of PAC-1, through the sequestration of inhibitory zinc. It should be noted that it is also possible that zinc is inhibiting caspase-3 in the cancer cell and that PAC-1, TPEN, and other zinc chelators induce apoptosis by relieving this inhibition of caspase-3. The *in vitro* data presented in Figs. 3, 4, and 5 indicate that PAC-1 does indeed activate zinc-inhibited caspase-3. Although in a number of cancer types the cellular procaspase-3/caspase-3 ratio is skewed heavily toward procaspase-3,<sup>21,24,64</sup> there is solid evidence in some cancer cell lines and primary isolates for the presence of significant levels of caspase-3.<sup>22,23,65,66</sup>

The results described herein have ramifications for the development of zinc chelators as anticancer agents and for the regulatory role played by zinc in apoptosis. As shown in Fig. 4a and b, PAC-1 actually inhibits caspase-3/procaspase-3 activity at high concentrations; thus, PAC-1 analogues that lack this effect (but still strongly chelate zinc) might be more potent proapoptotic agents. Furthermore, the addition of PAC-1 to caspase-3/procaspase-3 in Zn-containing buffer restores enzymatic activity to 40–60% of the levels in the absence of Zn (Fig. 4a–c); thus, it is possible that PAC-1 analogues that more fully activate caspase-3/procaspase-3 may be more potent anticancer agents. Finally, the data presented herein support the notion that cellular zinc plays an antiapoptotic role by inhibiting latent procaspase-3 activity. The identification of more potent versions of PAC-1, the evaluation of PAC-1 and derivatives in multiple animal models of cancer, and the role of zinc in procaspase-3 inhibition *in vivo* are all being actively investigated in our laboratory and the results will be presented in due course.

## Materials and Methods

### Materials

All reagents were obtained from Fisher unless otherwise indicated. All buffer solutions were made with Milli-Q purified water. PAC-1 and PAC-1a (Fig. 1a) were synthesized

as described.<sup>27</sup> Ac-DEVD-pNA was synthesized as described.<sup>67</sup> Luria broth (LB) was obtained from EMD. Etoposide was obtained from Sigma. Caspase Assay Buffer contains 50 mM Hepes (pH 7.4), 100 mM NaCl, 10 mM DTT, 0.1 mM EDTA disodium salt, 0.10% Chaps, 10% glycerol. Ni NTA Binding Buffer contains 50 mM Tris (pH 8.0), 300 mM NaCl, and 10 mM imidazole. Ni NTA Wash Buffer contains 50 mM Tris (pH 8.0), 300 mM NaCl, and 20 mM imidazole. Ni NTA Elution Buffer contains 50 mM Tris (pH 8.0), 300 mM NaCl, and 500 mM imidazole. The C-terminal 6×His-tagged procaspase-3 and procaspase-7 proteins were expressed and purified as described below. The 2× SDS sample buffer contains 100 mM Tris-Cl (pH 6.8), 200 mM DTT, 4% (w/v) SDS, 0.2% bromophenol blue, and 20% (v/v) glycerol.

### Strains and plasmids

Procaspase-3 and caspase-3 were expressed using the pHC332 expression plasmid. The uncleavable mutant (D9A/D28A/D175A) of procaspase-3 was created by successive quick-change mutations on pHC332 as previously described.<sup>30</sup> Procaspase-7 and caspase-7 were expressed from a pET23b plasmid. The uncleavable mutant (D23A/D198A/D206A) of procaspase-7 was created by successive quick-change mutations using the following primers: gcaaatgaagattcagtggtgctaagccagaccg for D23A, ggcatccaggccgctagcgggccatcaatg for D198A, and ccatcaatgacagcggcctaactctc for D206A.<sup>48</sup>

### Recombinant expression and purification of procaspase-3/-7

Expression of procaspase-3/-7 was preformed in the BL21(DE3) strain of *Escherichia coli* (Novagen) similar to that previously described.<sup>27</sup> Briefly, plasmids encoding for the C-terminally 6×His-tagged procaspase-3/-7 protein were transformed into electrocompetent BL21. The transformants were selected for by growth in ampicillin. Individual colonies were picked and used to inoculate 10-mL seed cultures of LB with ampicillin (100 µg/mL) for expression. Seed cultures were used to inoculate 2-L cultures of LB, which were grown at 37 °C to an OD<sub>600</sub>=0.6. Protein expression was induced via the addition of IPTG to a final concentration of 0.5 mM; after addition of IPTG, the culture was incubated at 37 °C with shaking for an additional 20 min. Bacterial cultures were then pelleted by centrifugation (at 5000g, 5 min, 4 °C) and lysed by pulse sonication on ice for 5 min in the presence of 30 mL Ni NTA binding buffer. Bacterial debris was removed by centrifugation (at 35,000g, 30 min, 4 °C) and the 6×His-tagged protein was purified from the supernatant with 1 mL 50% slurry Ni NTA resin (Qiagen). Protein was batch loaded onto the resin for 1 h at 4 °C. The bound resin was applied to a disposable column and the resin was washed with 15 mL of Ni NTA Wash Buffer. The protein was then eluted from the column with 10 mL of Ni NTA Elution Buffer. Fractions (~1 mL) were collected and the presence of protein was determined by reaction with the Bradford reagent (BioRad). Fractions containing protein were pooled and flash-frozen in liquid nitrogen. Protein was stored at -80 °C.

### Zinc-free preparation

Protein was expressed and purified as above until fractions were pooled. Protein was not flash-frozen at this

point, but fractions containing protein were pooled and applied to a PD-10 column (GE Healthcare) charged with Hepes buffer that had been treated with Chelex<sup>®</sup> resin. The Hepes buffer consisted of 50 mM Hepes and 300 mM NaCl (pH 7.4). The pH was monitored after treatment with the Chelex<sup>®</sup> resin and was found to have not changed. The protein was eluted using an additional 3.5 mL of Chelex<sup>®</sup>-treated Hepes buffer and the concentration was determined using the Edelhoch method for protein quantitation by absorbance at 280 nm. Protein isolated directly from the column typically had a concentration of ~50 µM; for experiments described herein requiring zinc-free conditions, the protein was typically diluted to the desired concentration in Hepes buffer that had been treated with Chelex<sup>®</sup> resin. Protein was flash-frozen in 500-µL aliquots in liquid nitrogen and stored at -80 °C.

### Expression of various caspase forms

Expression of procaspase-3, procaspase-3(D9A/D28A/D175A), procaspase-7, and procaspase-7(D23A/D198A/D206A) were performed as described above. Expression of caspase-3/-7 was performed as above except that the induction time with IPTG was for 4 h rather than 20 min. Purification and zinc-free preparations were performed in the same manner for all caspase forms.

### Buffer analysis

Aliquots of standard preparation of procaspase-3 were thawed and diluted to 500 nM in either Hepes, Tris buffer, or Chelex<sup>®</sup>-treated Tris buffer. A 45-µL volume of protein was added to each well of a 384-well plate. Vehicle or compound was added to each well to a final concentration of 50 µM. The plate was incubated at 37 °C for 2 h. A 5-µL volume of a 2 mM stock of Ac-DEVD-pNA was added to the plates to a final concentration of 200 µM. The absorbance of each well at 405 nm was monitored in a plate reader every minute for 60 min and the progress curve was plotted.

### Metal inhibition

Aliquots of zinc-free procaspase-3 were thawed and diluted to 500 nM in Chelex<sup>®</sup>-treated Hepes buffer. A 45-µL volume of a protein solution was added to each well of a 384-well plate. Various concentrations of different metals were added to each well and the plate was incubated for 2 h at 37 °C. A 5-µL volume of a 2 mM stock of Ac-DEVD-pNA was added to the plates to a final concentration of 200 µM. The absorbance of each well at 405 nm was monitored in a plate reader every minute for 60 min. The initial slope of each well was determined from the linear portion of the progress curve. This typically included all data points collected. The slopes were converted to a percent of the inhibition in the absence of metal and were plotted *versus* concentration. Data were generated in triplicate.

### Assay of Procaspase-3/-7 and Caspase-3/-7 Activity

Stocks of zinc-free enzyme were prepared with or without the appropriate amount of zinc and were incubated at room temperature for at least 30 min prior to addition to compound. Compound dilutions were made from the 10 mM dimethyl sulfoxide (DMSO) stock to the

appropriate concentration in the specified assay buffer and DMSO to maintain a constant amount of DMSO in every well (never above 5%). These were placed into wells of a 384-well plate (20  $\mu$ L), and then 25  $\mu$ L of an appropriately diluted enzyme stock in assay buffer was added to the compound wells (1  $\mu$ M procaspase-3, 1  $\mu$ M caspase-3, or 5  $\mu$ M D9A/D28A/D175A procaspase-3, 2  $\mu$ M procaspase-7, 2  $\mu$ M caspase-7, or 10  $\mu$ M D23A/D198A/D206A procaspase-7). Controls containing DMSO and assay buffer without compound or without both compound and enzyme were included for each experiment. For experiments in the presence of zinc, a control containing no zinc was also included. The plates were then incubated for 2 h at 37 °C. Then, to each well of the plate was added 5  $\mu$ L of a 2 mM stock of Ac-DEVD-pNA in assay buffer and the absorbance at 405 nm was read every minute for 1 h using a Spectra Max Plus 384 plate reader (Molecular Devices, Sunny Vale, CA). The slope of each well was used to determine the activity as compared to the controls. The data were plotted as percent activity *versus* compound concentration and fitted to a logistic dose-response curve using OriginPro (OriginLab Software, Northampton, MA) or Table Curve (SYSTAT Software, Richmond, CA) if appropriate. Data were generated in triplicate and repeated at least three times. The data presented are the average of the triplicate data points and is representative of the replicate experiments.

#### Assay of zinc inhibition of procaspase-3/7 and caspase-3/7 activity

Aliquots of frozen zinc-free protein were thawed and diluted in Hepes buffer (that had been treated with Chelex<sup>®</sup> resin) to the appropriate concentration. A 40- $\mu$ L solution of protein was added to each well of a 384-well plate and 5  $\mu$ L of various concentrations of zinc were added. Appropriate wells also received PAC-1 to a final concentration of 50  $\mu$ M. The plate was incubated at 37 °C for 2 h. A 5- $\mu$ L solution of a 2 mM stock of Ac-DEVD-pNA was added to each well to a final concentration of 200  $\mu$ M. The absorbance at 405 nm was monitored every minute for 60 min and the initial slope was determined from the linear portion of the progress curve. The slopes were converted to percent of maximal activity (the slope in the absence of zinc) and the data were fitted with a logistical dose-response curve. Data were generated in triplicate and repeated at least three times. The data presented are the averages of the triplicate data points and are representative of the replicate experiments.

#### SDS-PAGE analysis of caspase-3 activation

Aliquots of zinc-free caspase-3 and zinc-free procaspase-3 (C163A) were thawed and diluted to the appropriate concentration. A 22.5- $\mu$ L solution of each protein was added to each of fifteen 0.5-mL tubes. A 5- $\mu$ L solution of 500  $\mu$ M ZnSO<sub>4</sub> in Hepes buffer was added to 10 tubes to obtain a final ZnSO<sub>4</sub> concentration of 50  $\mu$ M. The remaining 5 tubes received 5  $\mu$ L of buffer. The appropriate compound was added (0.5  $\mu$ L of a 5 mM DMSO stock solution) to each tube and the final concentrations were 10  $\mu$ M caspase-3, 50  $\mu$ M procaspase-3 (C163A), 50  $\mu$ M ZnSO<sub>4</sub>, and 50  $\mu$ M compound. The tubes were incubated at 37 °C for up to 3 h. The reaction was stopped by the addition of 2 $\times$  SDS loading dye and boiling for 5 min. A 15- $\mu$ L volume of each sample was loaded on a 4–20% 15-well precast polyacrylamide gel (BioRad). The gel was run at 150 V for 45 min and stained with Coomassie brilliant

blue. The experiment was run three times each on two different batches of protein.

#### Western blot analysis of procaspase-3 activation

Aliquots of zinc-free procaspase-3 (D9A/D28A/D175A) and zinc-free procaspase-3 (C163A) were thawed and diluted to the appropriate concentration. A 22.5- $\mu$ L solution of each protein was added to each of twelve 0.5-mL tubes. A 5- $\mu$ L solution of 1 mM ZnSO<sub>4</sub> in Hepes buffer was added to nine tubes to obtain a final ZnSO<sub>4</sub> concentration of 100  $\mu$ M. The remaining three tubes received 5  $\mu$ L of buffer. The appropriate compound was added (0.5  $\mu$ L of a 5 mM DMSO stock solution) to each tube and the final concentrations were 10  $\mu$ M procaspase-3(D9A/D28A/D175A) and 50  $\mu$ M procaspase-3 (C163A); 100  $\mu$ M ZnSO<sub>4</sub> and 50  $\mu$ M compound were added to certain experiments as indicated in Fig. 6. The tubes were incubated at 37 °C for up to 12 h. The reaction was stopped by the addition of 2 $\times$  SDS loading dye and boiling for 5 min. A 15- $\mu$ L volume of each sample was loaded on a 4–20% 15-well precast polyacrylamide gel (BioRad). The gel was run at 150 V for 45 min and transferred to a PVDF membrane (Millipore) using a wet transfer method (40 V for 1 h). The blot was blocked in 10% milk in PBST for 4 h at 4 °C. The blot was then washed three times for 3 min with PBST to remove excess milk. The primary antibody (rabbit polyclonal) against the active fragments of caspase-3 (Calbiochem) was added at a dilution of 1:2000 and incubated at 4 °C for 4 h. The blot was then washed 2 times with PBST (PBS with Tween 20) and a 1:2000 dilution of a goat anti-rabbit Alexa Fluor 647-conjugated antibody was applied to the blot and allowed to incubate at 4 °C overnight. The blot was then washed three times with PBST and imaged on a Typhoon fluorescence scanner (Molecular Devices, Sunnyvale, CA). The experiment was repeated four times on two different batches of protein and the blot shown is representative of the results.

#### Zinc titration

Compounds were diluted from their 10 mM DMSO stocks into 3 mL of buffer A (50 mM Hepes, 100 mM KNO<sub>3</sub>, pH 7.4) to give a final concentration of 50  $\mu$ M in a quartz cuvette. The absorbance spectrum between 260 and 500 nm was then acquired using a Varian Carey 4000 Spectrophotometer (Palo Alto, CA). Then 5  $\mu$ L of a 3 mM ZnSO<sub>4</sub> solution in buffer A was added. The solution was mixed and allowed to equilibrate for 30 min. The absorbance spectrum was acquired again. This process was continued until the ZnSO<sub>4</sub> concentration had reached 75  $\mu$ M (addition of 75  $\mu$ L).

#### Continuous variations method

A series of buffer A solutions of PAC-1 and ZnSO<sub>4</sub> were prepared such that the sum of metal and ligand concentration was constant (50  $\mu$ M). The mole fraction of PAC-1 was varied between 0.1 and 1.0. A series of buffer A solutions of PAC-1 alone at the same concentrations was also prepared. A final set of solutions was prepared for maximal absorbance readings using 250  $\mu$ M PAC-1 with or without 25  $\mu$ M ZnSO<sub>4</sub>. In a 96-well plate, 200  $\mu$ L of each solution was added to different wells in triplicate. The absorbance at 410 nm was then acquired using a SpectraMax 384 plate reader (Molecular Devices). The maximal absorbance was calculated by subtraction of the

absorbance of 250  $\mu\text{M}$  PAC-1 alone from the absorbance of 250  $\mu\text{M}$  PAC-1 with 25  $\mu\text{M}$   $\text{ZnSO}_4$ . The normalized absorbance for each mole fraction was then calculated by subtracting the absorbance of PAC-1 at the appropriate concentration from the corresponding PAC-1/Zn mixed sample and dividing by the corrected maximal absorbance value. The normalized absorbance was then plotted *versus* mole fraction. The peak of the plot gives the stoichiometry of the interaction (based on the mole fraction) and was used to calculate the binding constant from the following equation (as  $y_{\text{max}}$ ):<sup>52</sup>

$$\log K_A = 0.3010 - \log[T] + \log y_{\text{max}} - 2\log(1 - y_{\text{max}})$$

### EGTA competition titration

In a quartz cuvette, a solution containing 32  $\mu\text{M}$  PAC-1 and 9.5  $\mu\text{M}$   $\text{ZnSO}_4$  in buffer A was titrated with 5- $\mu\text{L}$  aliquots of a 2.9 mM solution of EGTA in buffer A. Upon each addition of EGTA aliquot, the solution was allowed to equilibrate for 30 min prior to reading the absorbance spectrum between 260 and 500 nm on a Varian Carey 4000 spectrophotometer. The absorbance at 410 nm was used to calculate the [EGTA·Zn]. The absorbance data were first converted to the concentration of [PAC-1·Zn] using a calibration curve, then this value was subtracted from the total [Zn]. The plot of [EGTA·Zn] *versus* total [EGTA] was fit to the Hill equation using OriginPro (OriginLab Software). The  $K_D$  for PAC-1 was found by dividing the  $K$  from the fit by the  $K_D$  of EGTA ( $3.78 \times 10^8 \text{ M}^{-1}$ ).

### Cell death assays

U-937 cells were cultured in RPMI 1640 growth media with 10% fetal bovine serum and 1% Pen-Strep. One million cells were added to each well of a 12-well plate. Compound stocks in DMSO were added directly to the growth medium maintaining a constant amount of DMSO (<1%) in each well. Cells were incubated with compound at 37 °C and 5%  $\text{CO}_2$  for 24 h. After incubation with compound, cells were pelleted and the media was removed by aspiration. The cells were washed once in PBS. The cells were again pelleted and resuspended in 100  $\mu\text{L}$  of Annexin V binding buffer [10 mM Hepes (pH 7.4), 140 mM NaCl, 2.5 mM  $\text{CaCl}_2$ , 0.1% bovine serum albumin]. A 10- $\mu\text{L}$  solution of FITC-conjugated Annexin V was added to the cells and incubated on ice for 15 min. An additional 380  $\mu\text{L}$  of Annexin V binding buffer and a 10- $\mu\text{L}$  solution of a 1 mg/mL stock of propidium iodide was added to each sample. The cells were analyzed by flow cytometry and percent apoptosis was determined (Annexin V positive, PI negative). The experiment was performed three times and the average of each experiment is presented.

### Acknowledgements

We are grateful to the National Institutes of Health (R01-CA120439) for the support of this work. Q.P.P. was partially supported by a Chemistry–Biology Interface Training Grant from the National Institutes of Health (Ruth L. Kirschstein National Research Service Award 1 T32 GM070421 from the National Institute of General Medical Sciences). D.C.W. was

supported by Ruth L. Kirschstein National Research Service Award 3F31CA130138-01S1.

### Supplementary Data

Supplementary data associated with this article can be found, in the online version, at [doi:10.1016/j.jmb.2009.03.003](https://doi.org/10.1016/j.jmb.2009.03.003)

### References

- Papadopoulos, N., Kinzler, K. W. & Vogelstein, B. (2006). The role of companion diagnostics in the development and use of mutation-targeted cancer therapies. *Nat. Biotechnol.* **24**, 985–995.
- Hanahan, D. & Weinberg, R. A. (2000). The hallmarks of cancer. *Cell*, **100**, 57–70.
- Blatt, N. B. & Glick, G. D. (2001). Signaling pathways and effector mechanisms pre-programmed cell death. *Bioorg. Med. Chem.* **9**, 1371–1384.
- Fischer, U., Janicke, R. U. & Schulze-Osthoff, K. (2003). Many cuts to ruin: a comprehensive update of caspase substrates. *Cell Death Differ.* **10**, 76–100.
- Luthi, A. U. & Martin, S. J. (2007). The CASBAH: a searchable database of caspase substrates. *Cell Death Differ.* **14**, 641–650.
- Timmer, J. C. & Salvesen, G. S. (2007). Caspase substrates. *Cell Death Differ.* **14**, 66–72.
- Lowe, S. W., Cepero, E. & Evan, G. (2004). Intrinsic tumor suppression. *Nature*, **432**, 307–315.
- Igney, F. H. & Krammer, P. H. (2002). Death and anti-death: tumor resistance to apoptosis. *Nat. Rev. Cancer*, **2**, 277–288.
- Vogelstein, B. & Kinzler, K. W. (2001). Achilles' heel of cancer. *Nature*, **412**, 865–866.
- Kirkin, V., Joos, S. & Zornig, M. (2004). The role of Bcl-2 family members in tumorigenesis. *Biochim. Biophys. Acta*, **1644**, 229–249.
- Soengas, M. S., Capodici, P., Polsky, D., Mora, J., Esteller, M., Opitz-Araya, X. *et al.* (2001). Inactivation of the apoptosis effector Apaf-1 in malignant melanoma. *Nature*, **409**, 207–211.
- Bremer, E., van Dam, G., Kroesen, B. J., de Leij, L. & Helfrich, W. (2006). Targeted induction of apoptosis for cancer therapy: current progress and prospects. *Trends Mol. Med.* **12**, 382–393.
- Green, D. R. & Kroemer, G. (2005). Pharmacological manipulation of cell death: clinical applications in sight? *J. Clin. Invest.* **115**, 2610–2617.
- Fesik, S. W. (2005). Promoting apoptosis as a strategy for cancer drug discovery. *Nat. Rev. Cancer*, **5**, 876–885.
- Vassilev, L. T., Vu, B. T., Graves, B., Carvajal, D., Podlaski, F., Filipovic, Z. *et al.* (2004). In vivo activation of the p53 pathway by small-molecule antagonists of MDM2. *Science*, **303**, 844–848.
- Tovar, C., Rosinski, J., Filipovic, Z., Higgins, B., Kolinsky, K., Hilton, H. *et al.* (2006). Small-molecule MDM2 antagonists reveal aberrant p53 signaling in cancer: implications for therapy. *Proc. Natl Acad. Sci. USA*, **103**, 1888–1893.
- Oltersdorf, T., Elmore, S. W., Shoemaker, A. R., Armstrong, R. C., Augeri, D. J., Belli, B. A. *et al.* (2005). An inhibitor of Bcl-2 family proteins induces regression of solid tumours. *Nature*, **435**, 677–681.
- Nguyen, J. T. & Wells, J. A. (2003). Direct activation of the apoptosis machinery as a mechanism to

- target cancer cells. *Proc. Natl Acad. Sci. USA*, **100**, 7533–7538.
19. Li, L., Thomas, R. M., Suzuki, H., De Brabander, J. K., Wang, X. & Harran, P. G. (2004). A small molecule Smac mimic potentiates TRAIL- and TNF $\alpha$ -mediated cell death. *Science*, **305**, 1471–1474.
  20. Sun, H., Nikolovska-Coleska, Z., Yang, C. Y., Xu, L., Liu, M., Tomita, Y. *et al.* (2004). Structure-based design of potent, conformationally constrained Smac mimetics. *J. Am. Chem. Soc.* **126**, 16686–16687.
  21. Roy, S., Bayly, C. I., Gareau, Y., Houtzager, V. M., Kargman, S., Keen, S. L. C. *et al.* (2001). Maintenance of caspase-3 proenzyme dormancy by an intrinsic “safety catch” regulatory tripeptide. *Proc. Natl Acad. Sci. USA*, **98**, 6132–6137.
  22. Grigoriev, M. Y., Pozharissky, K. M., Hanson, K. P., Imyanitov, E. N. & Zhivotovsky, B. (2002). Expression of caspase-3 and -7 does not correlate with the extent of apoptosis in primary breast carcinomas. *Cell Cycle*, **1**, 337–342.
  23. O'Donovan, N., Crown, J., Stunell, H., Hill, A. D., McDermott, E., O'Higgins, N. & Duffy, M. J. (2003). Caspase 3 in breast cancer. *Clin. Cancer Res.* **9**, 738–742.
  24. Krepela, E., Prochazka, J., Liul, X., Fiala, P. & Kinkor, Z. (2004). Increased expression of Apaf-1 and procaspase-3 and the functionality of intrinsic apoptosis apparatus in non-small cell lung carcinoma. *Biol. Chem.* **385**, 153–168.
  25. Fink, D., Schlagbauer-Wadl, H., Selzer, E., Lucas, T., Wolff, K., Pehamberger, H. *et al.* (2001). Elevated procaspase levels in human melanoma. *Melanoma Res.* **11**, 385–393.
  26. Estrov, Z., Thall, P. F., Talpaz, M., Estey, E. H., Kantarjian, H. M., Andreeff, M. *et al.* (1998). Caspase 2 and caspase 3 protein levels as predictors of survival in acute myelogenous leukemia. *Blood*, **92**, 3090–3097.
  27. Putt, K. S., Chen, G. W., Pearson, J. M., Sandhorst, J. S., Hoagland, M. S., Kwon, J.-T. *et al.* (2006). Small molecule activation of procaspase-3 to caspase-3 as a personalized anticancer strategy. *Nat. Chem. Biol.* **2**, 543–550.
  28. Han, Z., Hendrickson, E. A., Bremner, T. A. & Wyche, J. H. (1997). A sequential two-step mechanism for the production of the mature p17:p12 form of caspase-3 *in vitro*. *J. Biol. Chem.* **272**, 13432–13436.
  29. Stennicke, H. R., Jurgensmeier, J. M., Shin, H., Deveraux, Q., Wolf, B. B., Yang, X. *et al.* (1998). Pro-caspase-3 is a major physiologic target of caspase-8. *J. Biol. Chem.* **273**, 27084–27090.
  30. Bose, K., Pop, C., Feeney, B. & Clark, A. C. (2003). An uncleavable procaspase-3 mutant has a lower catalytic efficiency but an active site similar to that of mature caspase-3. *Biochemistry*, **42**, 12298–12310.
  31. Feeney, B., Pop, C., Swartz, P., Mattos, C. & Clark, A. C. (2006). Role of loop bundle hydrogen bonds in the maturation and activity of (Pro)caspase-3. *Biochemistry*, **45**, 13249–13263.
  32. Perry, D. K., Smyth, M. J., Stennicke, H. R., Salvesen, G. S., Duriez, P., Poirier, G. G. & Hannun, Y. A. (1997). Zinc is a potent inhibitor of the apoptotic protease, caspase-3. A novel target for zinc in the inhibition of apoptosis. *J. Biol. Chem.* **272**, 18530–18533.
  33. Stennicke, H. R. & Salvesen, G. S. (1997). Biochemical characteristics of caspases-3, -6, -7, and -8. *J. Biol. Chem.* **272**, 25719–25723.
  34. Aiuchi, T., Mihara, S., Nakaya, M., Masuda, Y., Nakajo, S. & Nakaya, K. (1998). Zinc ions prevent processing of caspase-3 during apoptosis induced by geranylgeraniol in HL-60 cells. *J. Biochem. (Tokyo)*, **124**, 300–303.
  35. Chai, F., Truong-Tran, A. Q., Ho, L. H. & Zalewski, P. D. (1999). Regulation of caspase activation and apoptosis by cellular zinc fluxes and zinc deprivation: a review. *Immunol. Cell Biol.* **77**, 272–278.
  36. Maret, W., Jacob, C., Vallee, B. L. & Fischer, E. H. (1999). Inhibitory sites in enzymes: zinc removal and reactivation by thionein. *Proc. Natl Acad. Sci. USA*, **96**, 1936–1940.
  37. Charkoudian, L. K. & Franz, K. J. (2006). Fe(III)-coordination properties of neuromelanin components: 5,6-dihydroxyindole and 5,6-dihydroxyindole-2-carboxylic acid. *Inorg. Chem.* **45**, 3657–3664.
  38. Truong-Tran, A. Q., Grosser, D., Ruffin, R. E., Murgia, C. & Zalewski, P. D. (2003). Apoptosis in the normal and inflamed airway epithelium: role of zinc in epithelial protection and procaspase-3 regulation. *Biochem. Pharmacol.* **66**, 1459–1468.
  39. Shiozaki, E. N., Chai, J. & Shi, Y. (2002). Oligomerization and activation of caspase-9, induced by Apaf-1 CARD. *Proc. Natl Acad. Sci. USA*, **99**, 4197–4202.
  40. Zou, H., Yang, R., Hao, J., Wang, J., Sun, C., Fesik, S. W. *et al.* (2003). Regulation of the Apaf-1/caspase-9 apoptosome by caspase-3 and XIAP. *J. Biol. Chem.* **278**, 8091–8098.
  41. Chao, Y., Shiozaki, E. N., Srinivasula, S. M., Rigotti, D. J., Fairman, R. & Shi, Y. (2005). Engineering a dimeric caspase-9: a re-evaluation of the induced proximity model for caspase activation. *PLoS Biol.* **3**, e183.
  42. Shiozaki, E. N., Chai, J., Rigotti, D. J., Riedl, S. J., Li, P., Srinivasula, S. M. *et al.* (2003). Mechanism of XIAP-mediated inhibition of caspase-9. *Mol. Cell*, **11**, 519–527.
  43. Juan, T. S., McNiece, I. K., Argento, J. M., Jenkins, N. A., Gilbert, D. J., Copeland, N. G. & Fletcher, F. A. (1997). Identification and mapping of Casp7, a cysteine protease resembling CPP32 beta, interleukin-1 beta converting enzyme, and CED-3. *Genomics*, **40**, 86–93.
  44. Lippke, J. A., Gu, Y., Sarnecki, C., Caron, P. R. & Su, M. S. (1996). Identification and characterization of CPP32/Mch2 homolog 1, a novel cysteine protease similar to CPP32. *J. Biol. Chem.* **271**, 1825–1828.
  45. Fernandes-Alnemri, T., Armstrong, R. C., Krebs, J., Srinivasula, S. M., Wang, L., Bullrich, F. *et al.* (1996). *In vitro* activation of CPP32 and Mch3 by Mch4, a novel human apoptotic cysteine protease containing two FADD-like domains. *Proc. Natl Acad. Sci. USA*, **93**, 7464–7469.
  46. Stennicke, H. R. & Salvesen, G. S. (1999). Catalytic properties of the caspases. *Cell Death Differ.* **6**, 1054–1059.
  47. Shi, Y. (2004). Caspase activation, inhibition, and reactivation: a mechanistic view. *Protein Sci.* **13**, 1979–1987.
  48. Denault, J. -B. & Salvesen, G. S. (2003). Human caspase-7 activity and regulation by its N-terminal peptide. *J. Biol. Chem.* **278**; 34042–24050.
  49. Scott, F. L., Denault, J. B., Riedl, S. J., Shin, H., Renucci, M. & Salvesen, G. S. (2005). XIAP inhibits caspase-3 and -7 using two binding sites: evolutionarily conserved mechanism of IAPs. *EMBO J.* **24**, 645–655.
  50. Charkoudian, L. K., Pham, D. M. & Franz, K. J. (2006). A pro-chelator triggered by hydrogen peroxide inhibits iron-promoted hydroxyl radical formation. *J. Am. Chem. Soc.* **128**, 12424–12425.

51. Sivaramaiah, S. & Reddy, P. R. (2005). Direct and derivative spectrophotometric determination of zinc with 2,4-dihydroxybenzaldehyde isonicotinoyl hydrazone in potable water and pharmaceutical samples. *J. Anal. Chem.* **60**, 828–832.
52. Likussar, W. & Boltz, D. F. (1971). Theory of continuous variations plots and a new method for spectrophotometric determination of extraction and formation constants. *Anal. Chem.* **43**, 1265–1272.
53. Adair, G. S., Bock, A. B. & Field, H. (1925). The hemoglobin system. VI. The oxygen dissociation curve of hemoglobin. *J. Biol. Chem.* **63**, 259.
54. Fahrni, C. J. & O'Halloran, T. V. (1999). Aqueous coordination chemistry of quinoline-based fluorescence probes for the biological chemistry of zinc. *J. Am. Chem. Soc.* **121**, 11448–11458.
55. Carter, J. E., Truong-Tran, A. Q., Grosser, D., Ho, L., Ruffin, R. E. & Zalewski, P. D. (2002). Involvement of redox events in caspase activation in zinc-depleted airway epithelial cells. *Biochem. Biophys. Res. Commun.* **297**, 1062–1070.
56. Truong-Tran, A. Q., Carter, J., Ruffin, R. E. & Zalewski, P. D. (2001). The role of zinc in caspase activation and apoptotic cell death. *BioMetals*, **14**, 315–330.
57. Zhao, R., Planalp, R. P., Ma, R., Greene, B. T., Jones, B. T., Brechbiel, M. W. *et al.* (2004). Role of zinc and iron chelation in apoptosis mediated by tachpyridine, an anti-cancer iron chelator. *Biochem. Pharmacol.* **67**, 1677–1688.
58. Donadelli, M., Dalla Pozza, E., Costanzo, C., Scupoli, M. T., Scarpa, A. & Palmieri, M. (2008). Zinc depletion efficiently inhibits pancreatic cancer cell growth by increasing the ratio of antiproliferative/proliferative genes. *J. Cell. Biochem.* **104**, 202–212.
59. Hyun, H. J., Sohn, J. H., Ha, D. W., Ahn, Y. H., Koh, J. Y. & Yoon, Y. H. (2001). Depletion of intracellular zinc and copper with TPEN results in apoptosis of cultured human retinal pigment epithelial cells. *Invest. Ophthalmol. Vis. Sci.* **42**, 460–465.
60. Hyun, H. J., Sohn, J., Ahn, Y. H., Shin, H. C., Koh, J. Y. & Yoon, Y. H. (2000). Depletion of intracellular zinc induces macromolecule synthesis- and caspase-dependent apoptosis of cultured retinal cells. *Brain Res.* **869**, 39–48.
61. Truong-Tran, A. Q., Ruffin, R. E. & Zalewski, P. D. (2000). Visualization of labile zinc and its role in apoptosis of primary airway epithelial cells and cell lines. *Am. J. Physiol., Lung Cell. Mol. Physiol.* **279**, L1172–L1183.
62. Hashemi, M., Ghavami, S., Eshraghi, M., Booy, E. P. & Los, M. (2007). Cytotoxic effects of intra and extracellular zinc chelation on human breast cancer cells. *Eur. J. Pharmacol.* **557**, 9–19.
63. Zalewski, P. D., Forbes, I. J. & Betts, W. H. (1993). Correlation of apoptosis with change in intracellular labile Zn(II) using zinquin [(2-methyl-8-*p*-toluenesulphonamido-6-quinolyloxy)acetic acid], a new specific fluorescent probe for Zn(II). *Biochem. J.* **296** (Pt 2), 403–408.
64. Kania, J., Konturek, S. J., Marlicz, K., Hahn, E. G. & Konturek, P. C. (2003). Expression of survivin and caspase-3 in gastric cancer. *Dig. Dis. Sci.* **48**, 266–271.
65. Yang, S., Liu, J., Thor, A. D. & Yang, X. (2007). Caspase expression profile and functional activity in a panel of breast cancer cell lines. *Oncol. Rep.* **17**, 1229–1235.
66. Persad, R., Liu, C., Wu, T.-T., Houlihan, P. S., Hamilton, S. R., Diehl, A. M. & Rashid, A. (2004). Overexpression of caspase-3 in hepatocellular carcinomas. *Mod. Pathol.* **17**, 861–867.
67. Goode, D. R., Sharma, A. K. & Hergenrother, P. J. (2005). Using peptidic inhibitors to systematically probe the S1' site of caspase-3 and caspase-7. *Org. Lett.* **7**, 3529–3532.